nature medicine

Glycemic control in diabetes is restored by therapeutic manipulation of cytokines that regulate beta cell stress

Sumaira Z Hasnain[1], Danielle J Borg[2,7], Brooke E Harcourt[2,7], Hui Tong[1], Yonghua H Sheng[1], Choa Ping Ng[3], Indrajit Das[1], Ran Wang[1], Alice C-H Chen[1], Thomas Loudovaris[4], Thomas W Kay[4], Helen E Thomas[4], Jonathan P Whitehead[3,5], Josephine M Forbes[2,6], Johannes B Prins[3,6] & Michael A McGuckin[1,5,6]

In type 2 diabetes, hyperglycemia is present when an increased demand for insulin, typically due to insulin resistance, is not met as a result of progressive pancreatic beta cell dysfunction. This defect in beta cell activity is typically characterized by impaired insulin biosynthesis and secretion, usually accompanied by oxidative and endoplasmic reticulum (ER) stress. We demonstrate that multiple inflammatory cytokines elevated in diabetic pancreatic islets induce beta cell oxidative and ER stress, with interleukin-23 (IL-23), IL-24 and IL-33 being the most potent. Conversely, we show that islet-endogenous and exogenous IL-22, by regulating oxidative stress pathways, suppresses oxidative and ER stress caused by cytokines or glucolipotoxicity in mouse and human beta cells. In obese mice, antibody neutralization of IL-23 or IL-24 partially reduced beta cell ER stress and improved glucose tolerance, whereas IL-22 administration modulated oxidative stress regulatory genes in islets, suppressed ER stress and inflammation, promoted secretion of high-quality efficacious insulin and fully restored glucose homeostasis followed by restitution of insulin sensitivity. Thus, therapeutic manipulation of immune regulators of beta cell stress reverses the hyperglycemia central to diabetes pathology.

Type 2 diabetes mellitus (T2D) is characterized by the inability of pancreatic beta cells to secrete sufficient functional insulin to control blood glucose in the face of increased insulin resistance, which is typically associated with obesity[1]. Insulin synthesis begins in the ER, where preproinsulin is folded and then cleaved to form proinsulin, which moves to the Golgi and is packaged into granules, followed by cleavage to form mature insulin. Disturbances in insulin biosynthesis in the ER probably impair glucose homeostasis by reducing the efficacy of secreted insulin, including inappropriate secretion of proinsulin. Indeed, a characteristic manifestation of beta cell dysfunction is elevated serum proinsulin, which further impairs peripheral glucose uptake[1]. Protein misfolding within the ER, which results in ER stress, accompanies beta cell dysfunction in diabetes[2,3] and can be induced experimentally by high concentrations of glucose, non-esterified fatty acids (NEFAs) or proinflammatory cytokines, all of which cause beta cell oxidative stress[4]. The unfolded protein response (UPR), a network of signaling and transcriptional pathways invoked to resolve ER stress, is particularly important in secretory cells[2,5,6]. However, severe or prolonged ER stress can trigger inflammatory signaling[7,8] and promote the beta cell apoptosis characteristic of diabetes progression[9–12]. The UPR activates protein kinase RNA–like endoplasmic reticulum kinase (PERK), which inhibits translation, and activating transcription factor 6 (ATF6), which drives transcription of ER proteins. Another key element of the UPR is inositol-requiring protein 1 (IRE1), an endoribonuclease that splices the X-box protein 1 (XBP1) transcription factor mRNA (*Xbp1*), increasing ER capacity and removal of misfolded proteins[2,5]. Beta cell–specific *Xbp1* deficiency impairs proinsulin processing, decreases glucose-stimulated insulin secretion and increases serum proinsulin, resulting in hyperglycemia, thus phenocopying key features of T2D[13]. In beta cells experiencing UPR hyperactivation, PERK and IRE1 can induce IL-1β mRNA (*Il1b*), inflammasome activation and apoptosis via the thioredoxin-interacting protein (TXNIP)[14,15] and other mechanisms[12], although TXNIP does not mediate NEFA-induced apoptosis[16].

Beta cell ER stress in T2D pathophysiology is incompletely understood, and good therapeutic targets are lacking. Some inflammatory cytokines, including IL-1β, are known to induce ER and oxidative stress[9–11], and blockade of IL-1β has shown some efficacy in T2D[17–22]. We sought to identify inflammatory cytokines that modulate ER stress in the diabetic pancreas and test the hypothesis that manipulation of those cytokines would restore beta cell function and glycemic control.

RESULTS

Cytokine modulation of oxidative and ER stress

We used a direct measure of IRE1 activity, the ER stress–activated indicator (ERAI)-GFP reporter of *Xbp1* splicing[23], to screen a panel of

[1]Mucosal Diseases Group, Mater Research Institute–The University of Queensland, Translational Research Institute, Brisbane, Queensland, Australia. [2]Glycation & Diabetes Group, Mater Research Institute–The University of Queensland, Translational Research Institute, Brisbane, Queensland, Australia. [3]Metabolic Medicine Group, Mater Research Institute–The University of Queensland, Translational Research Institute, Brisbane, Queensland, Australia. [4]St. Vincent's Research Institute, Melbourne, Victoria, Australia. [5]School of Biomedical Sciences, University of Queensland, Brisbane, Queensland, Australia. [6]School of Medicine, University of Queensland, Brisbane, Queensland, Australia. [7]These authors contributed equally to this work. Correspondence should be addressed to M.A.M. (michael.mcguckin@mater.uq.edu.au).

Received 18 July; accepted 30 August; published online 2 November 2014; doi:10.1038/nm.3705

cytokines for induction of ER stress in mouse MIN6N8 insulinoma–derived beta cells. IL-23, IL-24 and IL-33 were potent inducers of ER stress and IL-1β, macrophage inflammatory protein-2α, IL-17A, interferon-γ (IFN-γ) and IFN-β caused milder ER stress, whereas the other cytokines had negligible effect (**Fig. 1a**). By assessing *Xbp1* splicing, ATF6 nuclear translocation and eukaryotic initiation factor-2α phosphorylation we demonstrated activation of all major arms of the UPR and found that IL-23 and IL-24 progressively intensified ER stress over 36 h of exogenous treatment (**Supplementary Fig. 1a**,**b**). All ER stress–inducing cytokines triggered production of reactive oxygen species (ROS) and nitrite (a stable metabolite of nitric oxide) (**Supplementary Fig. 2**). Using pharmacological oxidative stress inhibitors, as well as inhibitors and siRNA for downstream signal transducers, we showed that each cytokine induced ER stress via oxidative stress generated in response to specific transcription factors (**Supplementary Table 1** and **Supplementary Fig. 3**). For example, IL-23 acted via signal transducer and activator of transcription 3 (STAT3), IL-24 acted via STAT1 and IL-33 required both STAT5 and nuclear factor κ-light-chain-enhancer of activated B cells (NF-κB).

By exposing beta cells to pairwise combinations of cytokines we found that IL-22 and IL-10 inhibit ER stress initiated by cytokines or the N-glycosylation inhibitor tunicamycin, with IL-22 being the most potent (**Fig. 1b**). IL-22 also inhibited ER stress induced with palmitic acid (**Fig. 1c**), a NEFA that induces beta cell oxidative and ER stress[24]. IL-22 alone did not activate the UPR. However, when ER stress was induced with thapsigargin, which depletes Ca^{2+} from the ER, IL-22 increased UPR activation (**Fig. 1c**). IL-22 completely abrogated further *Xbp1* splicing within 4–6 h when concomitantly administered with ER stressors (**Supplementary Fig. 1b**). Treatment with siRNA to silence both *Stat1* and *Stat3* was required to block IL-22–mediated suppression of ER stress (**Fig. 1d**). IL-22–mediated suppression of beta cell ER stress was completely inhibited by an IL-22 receptor (IL-22R1) neutralizing antibody (**Fig. 1e**), and IL-22R1 was highly expressed in mouse beta cells (**Fig. 1f**), as reported in humans[25].

Given that all of the ER stressors inhibited by IL-22 induce oxidative stress, we hypothesized that IL-22 inhibits oxidative stress. Over a 30-min exposure in MIN6N8 cells, IL-23 rapidly and progressively induced oxidation of a fluorescent dye (dihydroethidium, DHE) activated by O_2^-. DHE oxidation was lower in cells concomitantly incubated with IL-22, whereas a 30-min pre-exposure to IL-22 completely prevented DHE oxidation by IL-23 (**Fig. 1g** and **Supplementary Videos 1**–**4**). IL-22 potently repressed the production and accumulation of ROS and nitrite in beta cells in response to inflammatory cytokines, NEFAs, tunicamycin or H_2O_2, and basal nitrite production was lower in unstressed IL-22–treated cells (**Fig. 1h** and **Supplementary Fig. 2**). Given that IL-22 acted via transcription factors, we used an RT-PCR array to assess changes in expression of oxidative stress pathway genes in nonstressed beta cells treated with IL-22 (**Supplementary Fig. 4a**,**b**) and confirmed candidate genes by quantitative RT-PCR (qRT-PCR) (**Fig. 1i** and **Supplementary Fig. 4c**). IL-22 downregulated three key oxidative stress inducing genes: *Nos2* (encoding nitric oxide synthase-2, or iNos), *Hsp90ab1* (encoding mitochondrial heat shock protein) and *Fth1* (encoding ferritin heavy chain-1). Concomitantly, IL-22 upregulated the antioxidant genes *Gpx5* (encoding glutathione peroxidase-5), *Prdx5* (encoding peroxiredoxin-5) and *Sod2* (encoding superoxide dismutase-2), the cyclooxygenase genes *Ptgs1* and *Ptgs2* (encoding COX-1 and COX-2) and *Cyba* (encoding the $p22^{phox}$ regulatory component of NADPH oxidase).

IL-22 modulates islet ER stress and insulin secretion

We treated healthy mouse islets with tunicamycin, thapsigargin, IL-1β, IL-23 or IL-24, which resulted in induction of *Xbp1* splicing and expression of *Hspa5* mRNA (which encodes 78 kDa glucose-regulated protein, Grp78, an ER chaperone upregulated during ER stress), confirming that IL-23 and IL-24 are potent islet ER stressors (**Fig. 2a**). *In vivo*, insulin secretion is regulated by both meal-derived glucose and by the incretin glucagon-like peptide-1 (GLP-1), which is secreted postprandially. Consistent with UPR-mediated suppression of insulin translation and secretion[6,26], each ER stressor inhibited both glucose-stimulated and glucose- and GLP-1–stimulated total insulin (insulin plus proinsulin) secretion (GSIS and GLP-1–GSIS respectively; **Fig. 2b**). Co-treatment with IL-22 substantially prevented ER stress (**Fig. 2a**) and restored GSIS and GLP-1–GSIS (**Fig. 2b**). The ER stressors also resulted in modest proinsulin secretion in response to glucose and GLP-1 that was prevented by IL-22 (**Fig. 2c**). IL-22 did not prevent ER stress or the impaired insulin secretion caused by thapsigargin (**Fig. 2a**–**c**).

Healthy mouse islets treated *ex vivo* with IL-22R1–blocking antibody had higher ER stress, lower expression of antioxidant genes, higher *Nos2* expression (**Fig. 2d**) and lower GSIS (**Fig. 2e**). Islets from mice with high-fat diet–induced obesity (HFDIO) had higher ER stress and higher expression of antioxidant genes and *Nos2* than islets from mice fed normal chow (**Fig. 2d**). In comparison, HFDIO islets cultured with IL-22 had lower ER stress, higher antioxidant gene expression and lower *Nos2* expression (**Fig. 2d**). In contrast to acute ER stress, islets from HFDIO mice, whose islets are adapted to chronic ER stress, showed higher GSIS than healthy islets. Insulin hypersecretion was accentuated by culture with IL-22R1–neutralizing antibody, whereas after culture in IL-22 secretion was similar to the rate in islets from nonobese mice (**Fig. 2f**). Islets from HFDIO mice, but not those from lean mice, secreted proinsulin, even in low glucose conditions, but we did not detect proinsulin secretion in IL-22–treated islets from HFDIO mice (**Fig. 2g**).

Increased ER stress modulating cytokines in diabetic islets

Although the most potent beta cell ER stressors, IL-23, IL-24 and IL-33, have not been previously implicated in T2D pathogenesis, their mRNA expression was higher in pancreatic islets from mice with HFDIO (**Fig. 3a**) and those from mice with diabetes due to leptin receptor deficiency (**Fig. 3c**). The IL-22–regulated pro-oxidant genes and antioxidant genes also showed higher mRNA expression in islets from both models of obesity (**Fig. 3b**,**d**).

IL24 and *IL33* were the most highly upregulated ER stress–modulating cytokine genes in our analysis of a large transcriptome study comparing human healthy and T2D islets[27], demonstrating the clinical relevance of these cytokines (**Supplementary Table 2**).

Cytokine modulation improves glycemic control in obese mice

Our *in vitro* findings suggested that neutralizing the ER stressor cytokines or administering IL-22 would reduce pancreatic oxidative and ER stress and improve insulin biosynthesis in obesity. In mice fed an HFD for 15 weeks, administration of IL-22, or neutralizing antibodies to IL-23 or IL-24 after 12 weeks of the diet, substantially reversed glucose intolerance as measured by an intraperitoneal (i.p.) glucose tolerance test (IPGTT), with IL-22 being the most efficacious (**Fig. 4a**–**c**). The area under the curve (AUC glucose) for the IPGTT was 2.5-fold higher in mice with HFDIO than in normal chow–fed mice, and the mean difference was 42%, 50% and 82% lower with anti–IL-23, anti–IL-24 and IL-22 treatment, respectively. Improved

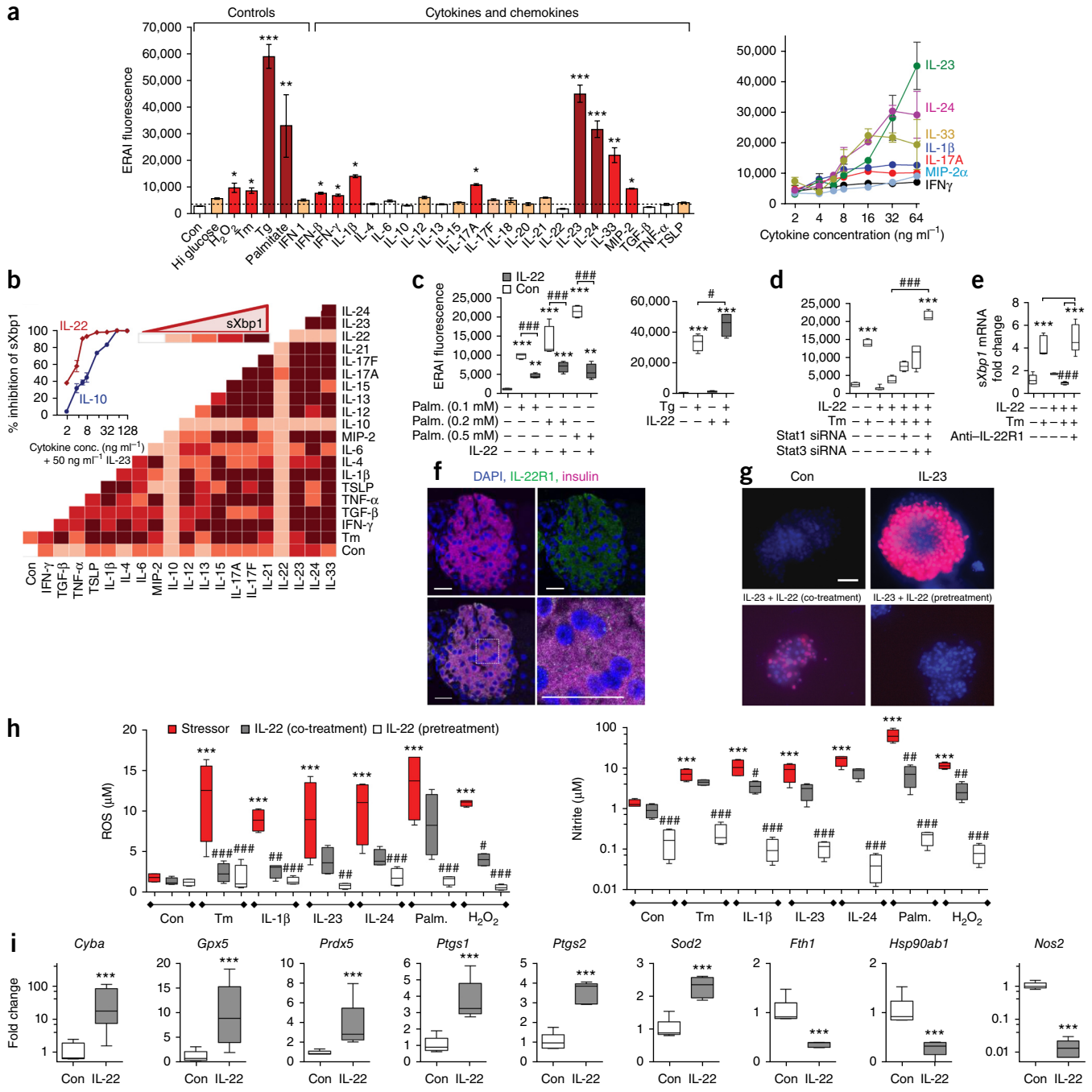

Figure 1 Cytokines regulate oxidative and ER stress in mouse MIN6N8 insulinoma beta cells. (**a–d**) ERAI-XBP1 reporter fluorescence in MIN6N8 cells cultured in 5.5 mM glucose for 48 h before 24 h with either 16.6 mM glucose (Hi glucose), or in 5.5 mM glucose with 10 μM H_2O_2, 0.5 mM palmitic acid or 50 ng ml^{-1} cytokines, or 6 h treatment with 10 μg ml^{-1} tunicamycin (Tm) or 5 μM thapsigargin (Tg) (right graph shows dose response) (**a**), pairwise combinations of cytokines or Tm as in **a**, shown as heat map with inset showing IL-10 and IL-22 dose response for suppression of IL-23-induced ERAI (**b**), 0.1–0.5 mM palmitic acid (left, 24 h) or 5 μM Tg (right, 6 h) ± 50 ng ml^{-1} IL-22 (**c**) and IL-22, Tm or both for 6 h as per **a** in cells transfected with control siRNA or siRNA for *Stat1*, *Stat3* or both (**d**). (**e**) Xbp1 splicing (s*Xbp1*) assessed by qRT-PCR (fold of control) after treatment of MIN6N8 cells with Tm ± IL-22 ± anti–IL-22R1 antibody for 6 h. (**f**) Pancreatic IL-22R1 and insulin expression in healthy mice by immunofluorescence and confocal microscopy; representative of 8 mice; scale bars, 50 μm; bottom right image is an enlargement of the boxed area in the bottom left image. (**g**) Confocal micrographs of MIN6N8 cells loaded with dihydroethidium (fluoresces red after oxidation) exposed to 50 ng ml^{-1} IL-23 for 30 min ± 50 ng ml^{-1} IL-22 at the same time or 30 min before IL-23, representative of 4 replicate cultures; DAPI (blue) stained nuclei; scale bar, 100 μm. (**h**) Concentration of ROS and nitrite at the peak time of production (30 min, 2 h or 8 h) in MIN6N8 cells treated with Tm, cytokines, palmitic acid or H_2O_2 at the doses in **a** ± 50 ng ml^{-1} IL-22 (co-treatment or 30-min pretreatment). (**i**) Oxidative stress gene expression in MIN6N8 cells ± 8 h exposure to 50 ng ml^{-1} IL-22; qRT-PCR as in **e**. MIP-2, macrophage inflammatory protein 2; TGF-β, transforming growth factor-β; TNF-α, tumor necrosis factor-α; TSLP, thymic stromal lymphopoietin. In **a–e**,**h**,**i**: Con, vehicle control (either 0.1% DMSO (**a–c** right graph, **d–f**,**g**,**i**) or 0.5% NEFA-free BSA (**c** left graph, **h**)). Box plots show median, interquartile range (IQR) and range; histograms show mean ± s.e.m. in **a** $n = 12$ for all conditions except palmitate, H_2O_2 and dose response curves ($n = 8$) and Tg, IFN1, IFN-β, IL-18 and IL-20 ($n = 6$); in **b** $n = 4$; in **c–e**,**h**,**i**, $n = 4$ replicate cultures; analysis of variance (ANOVA), Bonferroni's *post hoc* test; $^{*,\#}P < 0.05$, $^{**,\#\#}P < 0.01$, $^{***,\#\#\#}P < 0.001$ (from *post hoc* test); * versus untreated vehicle control, # versus stressor without IL-22, or as shown by bar.

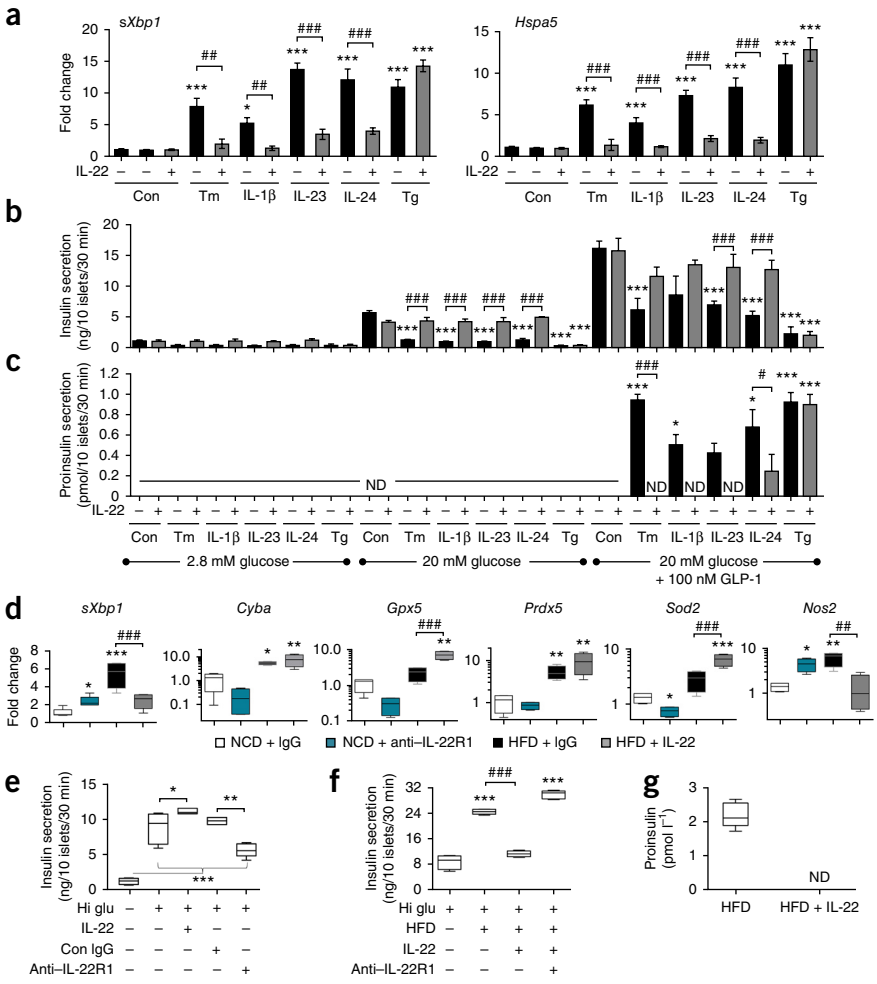

Figure 2 Cytokine-regulated oxidative and ER stress affects islet insulin secretion. (**a**–**c**) Xbp1 splicing (s*Xbp1*) and *Hspa5* mRNA expression (**a**) and insulin (**b**) and proinsulin (**c**) secretion from healthy islets cultured in 5.5 mM glucose with tunicamycin (Tm, 10 μg ml^{-1}) or thapsigargin (Tg, 5 μM) ± IL-22 for 6 h or ER stress-inducing cytokines ± IL-22 for 24 h and then cultured consecutively for 30 min in 2.8 mM glucose, 20 mM glucose and 20 mM glucose + 100 nM GLP-1. (**d**) mRNA expression of oxidative and ER stress genes in healthy islets cultured for 24 h in 5.5 mM glucose with 10 μg ml^{-1} control (IgG) or anti–IL-22R1 antibodies and in islets from mice on a HFD for 20 weeks cultured for 24 h in control IgG or IL-22. (**e**,**f**) Total insulin secretion in 30 min by islets from mice fed normal chow diet (NCD) or HFD cultured ± 20 mM glucose (Hi glu) following 24 h culture in 5.5 mM glucose ± IgG or anti–IL-22R1. (**e**) or following 24 h culture in 5.5 mM glucose ± IL-22 ± anti-IL-22R1 (**f**). (**g**) Proinsulin secretion by HFD islets in 5.5 mM glucose ± IL-22. In **a**–**g**: cytokines 50 ng ml^{-1}, antibodies 10 μg ml^{-1}. ND, not detected, below the lower limit of assay sensitivity. Con, vehicle control, 0.1% DMSO. In **a**,**d**, fold change from control. Statistics: histograms show mean ± s.e.m.; box plots show median, IQR and range; in **a**–**c**, $n = 4$ (compiled from two distinct experiments); in **d**, $n = 5$ (*sXbp1*) or $n = 4$ (all other genes); **e**–**g**, $n = 5$ mice; in **d**–**g**, $n = 5$ or 6 mice; ANOVA with Bonferroni's *post hoc* test; $^{*,\#}P < 0.05$, $^{**,\#\#}P < 0.01$, $^{***,\#\#\#}P < 0.001$ (from *post hoc* test); * versus untreated vehicle control, # as shown.

glucose tolerance could occur via improved insulin sensitivity; however, insulin tolerance tests (ITTs) showed that treated obese mice had unresolved insulin resistance (**Fig. 4a**–**c** and **Supplementary Table 3**). Fasted total insulin concentrations and the AUC insulin in the IPGTT were lower after all three therapies; however, the AUCs for insulin were greater than in mice fed normal chow (**Fig. 4a**–**c**). The fasted serum proinsulin-insulin ratio was lower in anti–IL-23– and IL-22–treated obese mice (**Fig. 4d**), with mean serum proinsulin 92% lower in IL-22–treated mice compared to IgG-treated obese mice by the end of the 3-week treatment (**Supplementary Table 3**).

Improvements in glycemic control were paralleled by lower total pancreatic ER stress consistent with alleviation of ER stress in the predominant exocrine pancreas (**Fig. 4e** and

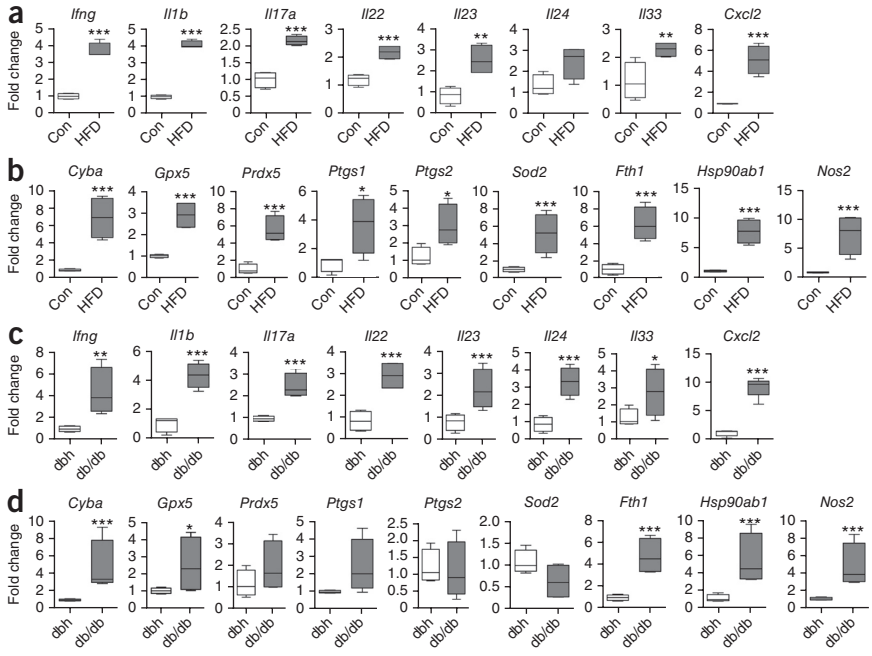

Figure 3 Inflammation and oxidative stress gene expression in mouse obesity and diabetes. (**a**–**d**) Cytokine and chemokine gene (**a**,**c**) and oxidative stress regulatory gene (**b**,**d**) mRNA expression in islets from mice fed normal chow (Con) or a 20-week HFD (**a**,**b**) or leptin receptor–deficient (db/db) versus heterozygous (dbh) littermates at 20 weeks of age (**c**,**d**). Data are fold over Con or dbh. Statistics: box plots show median, IQR and range; in **a**–**d**, $n = 4$ mice except in **c** for *Cxcl2*, $n = 5$ mice; *t*-test; $^{*}P < 0.05$, $^{**}P < 0.01$, $^{***}P < 0.001$ versus Con (**a**,**b**) or dbh (**c**,**d**).

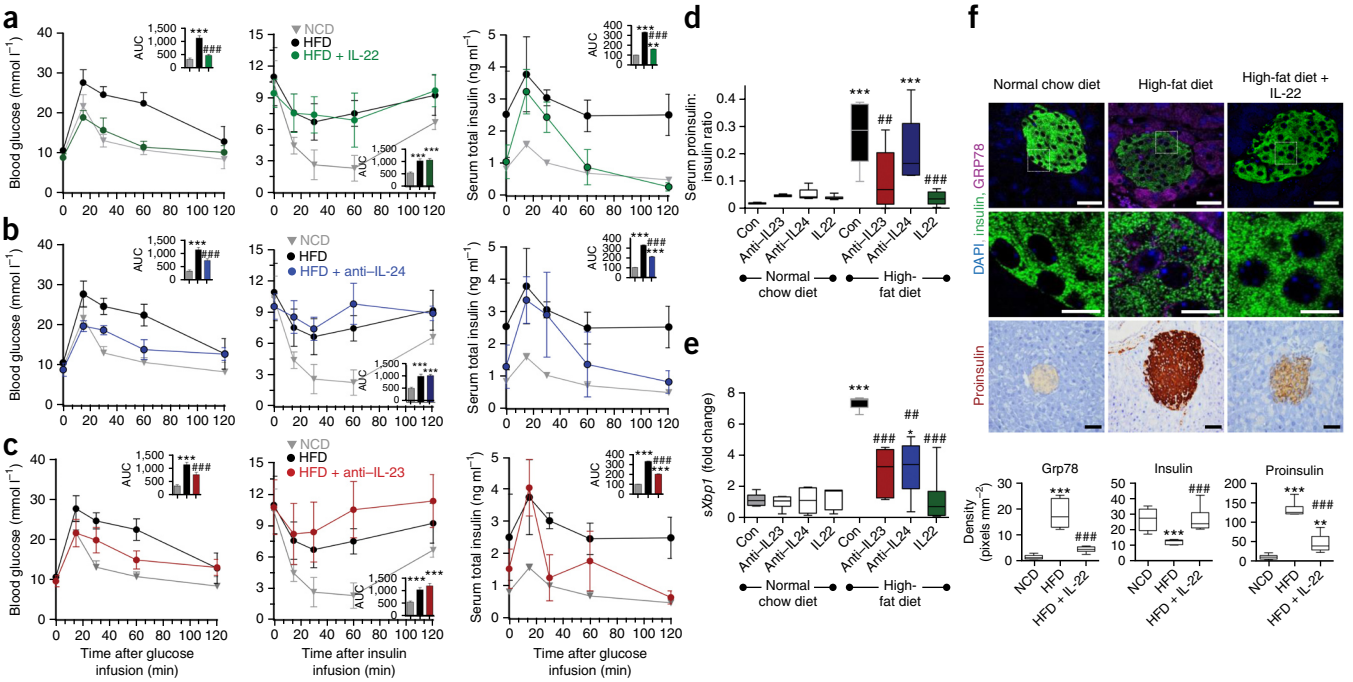

Figure 4 Targeting cytokine-induced ER stress in HFDIO improves glucose tolerance and hyperinsulinemia. (**a**–**c**) Mice were fed a HFD or normal chow diet (NCD) for 16 weeks and treated for the last 3 weeks with IL-22 (20 ng g^{-1} i.p. twice weekly) (**a**), anti–IL-24 (0.1 mg per mouse i.p. weekly) (**b**) or anti-IL-23 (3 µg g^{-1} i.p. weekly) (**c**). NCD and HFD control mice received an irrelevant IgG control antibody. Blood glucose (left) and serum total insulin (right) during fasted i.p. glucose tolerance tests on treatment day 14 and blood glucose during insulin tolerance tests on day 16 (middle). **d–f** are samples after 3 weeks treatment. (**d**) Fasting serum proinsulin:insulin ratio. (**e**) Total pancreatic spliced Xbp1 (s*Xbp1*) mRNA (fold of NCD IgG control). (**f**) Co-staining of pancreas for total insulin and Grp78 analyzed by confocal microscopy (top) and immunohistochemical staining of proinsulin (bottom). Graphs show quantitation of islet staining. Scale bars: top and bottom images, 50 µm; middle images, 10 µm. Middle images are enlargements of the boxed areas in the top images. Statistics: in **a–c**, mean ± s.e.m.; in **d–f**, box plots show median, IQR and range; in **a**–**c**, $n = 5$ randomly selected subset of IgG-treated NCD ($n = 6$), IgG-treated HFD ($n = 6$), anti–IL-23–treated HFD ($n = 8$), anti–IL-24–treated HFD ($n = 6$) and IL-22–treated HFD ($n = 9$) mice shown in **d–f**; ANOVA, Bonferroni's *post hoc* test; versus untreated *NCD and #HFD; $^{*}P < 0.05$, $^{**,\#\#}P < 0.01$, $^{***,\#\#\#}P < 0.001$ (from *post hoc* test); versus irrelevant antibody *NCD and #HFD controls.

Supplementary Fig. 5a). Immunostaining for Grp78, which accumulates with misfolded proteins, was 11.2-fold higher in the beta cell region of islets from HFDIO mice versus those from nonobese mice and was 75% lower in islets from IL-22–treated obese mice (**Fig. 4f**). Grp78 also accumulated in alpha cells and exocrine acinar cells in HFDIO mice (**Supplementary Fig. 5b**). Beta cell insulin stores in HFDIO were 53% lower than in nonobese mice, whereas insulin stores in IL-22–treated obese mice were similar to those in nonobese mice versus IgG-treated obese mice (**Fig. 4f**). Conversely, proinsulin abundance was 10.4-fold higher in islets from HFDIO mice compared to those from nonobese mice and 64% lower in islets from IL-22–treated obese mice versus IgG-treated obese mice (**Fig. 4f**). Total pancreatic *Ins2* mRNA expression was not substantially altered by the diet or treatments, with the exception of slightly lower expression in IL-22–treated obese compared IgG-treated obese mice (**Supplementary Fig. 5c**). In parallel, obese mice treated with the cytokine-neutralizing antibodies and IL-22 had lower expression of pancreatic inflammatory genes (**Supplementary Fig. 5d**).

HFD-fed mice treated with IL-22, but not mice treated with IL-23– or IL-24–neutralizing antibodies, progressively lost weight during treatment without changing food consumption (**Supplementary Fig. 6a**,**b**). Normal chow–fed mice did not show any significant change in weight or metabolic measurements after IL-22 therapy, although there were trends toward lower fasted blood glucose and insulin concentrations (**Supplementary Table 3**) and improved glucose tolerance with IL-22 (**Supplementary Fig. 6a**). IL-22 also affects hepatocytes[28], and hepatic ER stress occurs in obesity[29]. Whereas hepatic *Xbp1* splicing was only slightly higher in HFDIO mice, *Hspa5* expression was highly upregulated in the livers of HFDIO mice and was substantially lower in obese mice treated with anti–IL-23, anti–IL-24 and IL-22 (**Supplementary Fig. 6c**,**d**).

IL-22 therapy resolves islet pathophysiology in obesity

To assess longer and higher dose therapy in more advanced disease, we administered IL-22 at 20 (the first experiment dose) or 100 ng per g body weight (ng g^{-1}) to mice twice weekly for the last 30 d of a 22-week HFD regimen. Mean body weight decreased by 8.8% and 3.1% in obese mice treated with 20 and 100 ng g^{-1} IL-22, respectively, beginning ~1 week into treatment, compared to a 13.2% increase in IgG-treated obese mice (**Fig. 5a**). Weight changes were accompanied by altered distribution of adipose tissue, with more epididymal and brown fat in IL-22–treated mice (**Supplementary Fig. 7a**). Random-fed blood glucose decreased to concentrations seen in normal chow–fed mice within 7 d with both doses of IL-22 (**Fig. 5a**). An IPGTT on day 25 of therapy showed glycemic control indistinguishable from that of control nonobese mice (**Fig. 5a**). At day 16 of therapy, an ITT showed no or modest improvement in insulin resistance in IL-22–treated versus IgG-treated obese mice; however, by day 29, insulin resistance was lower in mice treated with both doses of IL-22 (**Fig. 5a**). IL-22–treated obese mice had normal fasting serum insulin and normalized GSIS by the IPGTT on day 25 (**Fig. 5a**). These improvements were accompanied by normalization of the serum proinsulin-insulin ratio, with serum proinsulin 97% lower in HFDIO

mice treated with 100 ng g^{-1} IL-22 than in IgG-treated mice (**Fig. 5b** and **Supplementary Table 3**).

Fasted serum glucagon did not change with the HFD regimen or after IL-22 treatment (**Supplementary Fig. 7b**). The dose-dependent improvement in serum proinsulin was mirrored by lower proinsulin staining and higher total insulin staining of islets from IL-22–treated obese mice (**Supplementary Fig. 7c**). Insulin (*Ins2*) islet mRNA expression did not change in control IgG–treated mice with HFDIO or in obese mice treated with IL-22, whereas expression of *Mafa*, encoding a transcription factor that drives beta cell secretory gene expression, trended higher with the HFD but was not altered by IL-22 treatment (**Supplementary Fig. 7d**). Also, despite the

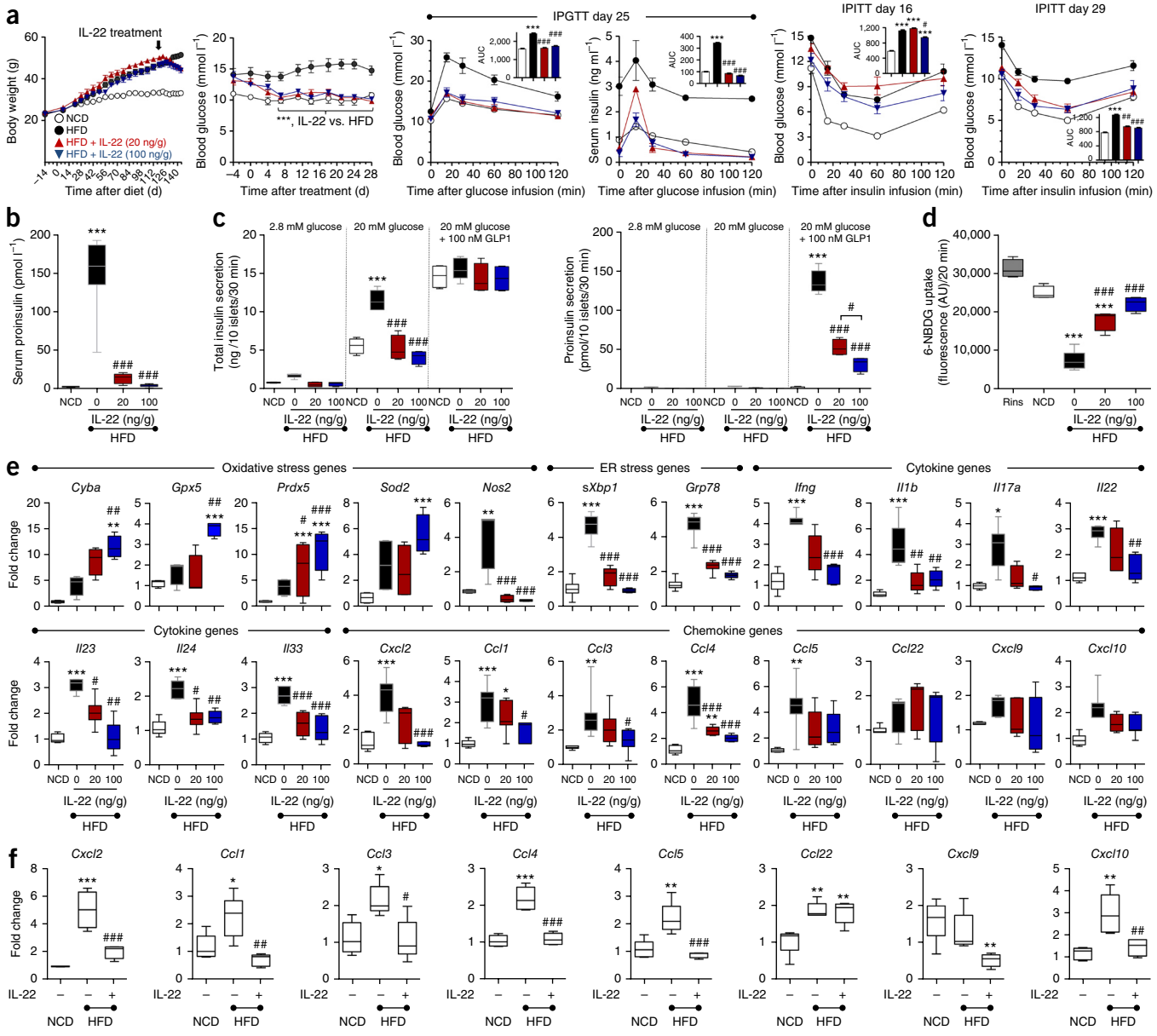

Figure 5 Extended IL-22 treatment in HFDIO restores glucose tolerance and insulin sensitivity, normalizes islet insulin secretion and suppresses oxidative stress, ER stress and inflammation. (**a**–**e**) Mice were fed a HFD or normal chow diet (NCD) for 22 weeks and treated for the last 30 d with 20 or 100 ng g^{-1} IL-22 i.p. twice weekly. NCD and HFD control mice received control IgG. (**a**) Body weight and random fed blood glucose concentrations. Blood glucose and insulin during a fasted i.p. glucose tolerance test on day 25 and insulin tolerance tests on days 16 and 29 of treatment. (**b**) Fasted serum proinsulin on day 30. (**c**) Total insulin and proinsulin secretion from islets sampled on day 30, cultured overnight in 5.5 mM glucose then consecutively for 30 min each with 2.8 mM glucose, 20 mM glucose and 20 mM glucose + 100 nM GLP-1. (**d**) Uptake of fluorescent 6-NBDG by 3T3 adipocytes in response to 2 ng ml^{-1} of recombinant insulin (Rins) or insulin derived from the glucose plus GLP-1 stimulation of islets shown in **c**. AU, arbitrary units. (**e**) Pancreatic islet mRNA expression of oxidative stress, ER stress, cytokine and chemokine genes. (**f**) Chemokine mRNA expression in islets from mice on a HFD or NCD for 20 weeks, cultured for 24 h in 5.5 mM glucose ± 50 ng ml^{-1} IL-22. In **e**,**f**, fold of NCD control. Statistics: in **a**: mean ± s.e.m.; in **b**–**f**, box plots show median, IQR and range. In **a**,**b**, $n = 12$ mice except IgG-treated NCD ($n = 8$) and IPGTT and IPITT ($n = 6$); in **c**, $n = 4$ mice except IgG-treated HFD ($n = 5$) were a randomly selected subset; in **d**, $n = 4$ mice were a randomly selected subset; in **e**, chemokine genes $n = 7$ mice, cytokine genes $n = 6$ mice, ER stress genes $n = 6$ mice, oxidative stress genes $n = 4$ mice; in **f**, $n = 5$ mice except Cxcl2 ($n = 4$).In **a**,**b**, $n = 12$ except IPGTT and IPITT ($n = 6$); in **c**,**d**, $n = 5$ or 6 were a randomly selected subset; in **e**, $n = 7$–10 mice; in **f**, $n = 4$–6 mice. ANOVA, Bonferroni's *post hoc* test; $^{*,\#}P < 0.05$, $^{**,\#\#}P < 0.01$, $^{***,\#\#\#}P < 0.001$ (from *post hoc* test); versus irrelevant antibody treated *NCD and $^{\#}$HFD controls, or as shown by bar.

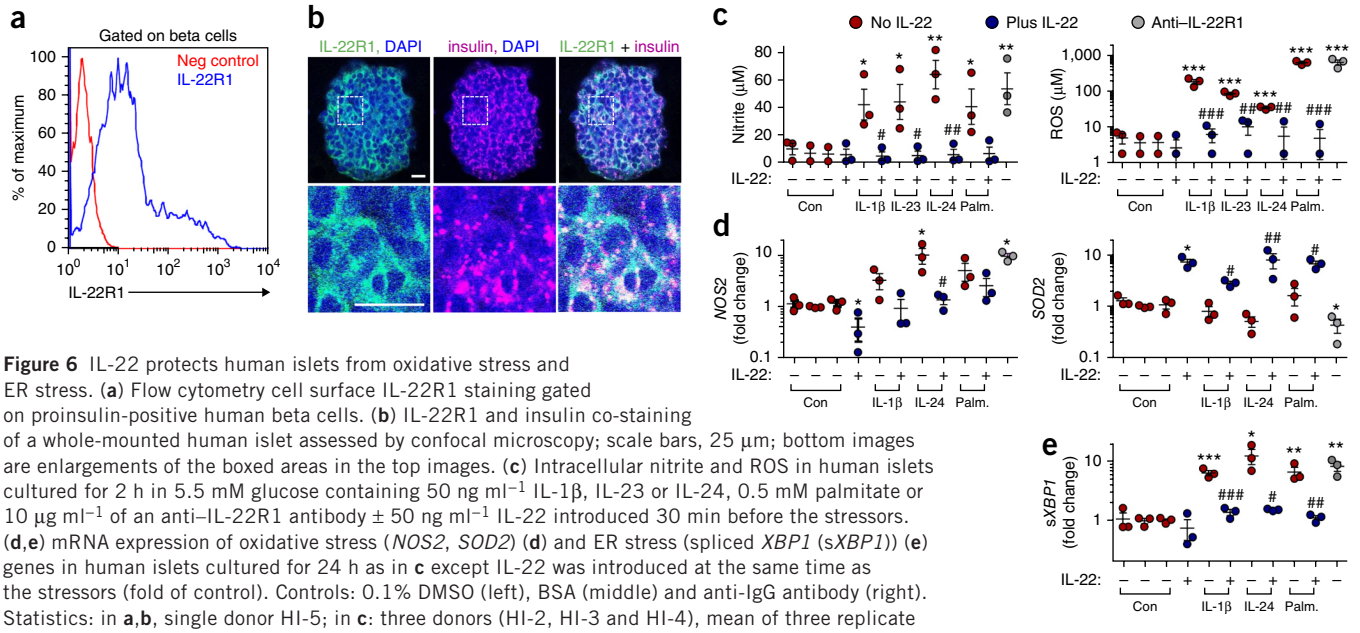

Figure 6 IL-22 protects human islets from oxidative stress and ER stress. (**a**) Flow cytometry cell surface IL-22R1 staining gated on proinsulin-positive human beta cells. (**b**) IL-22R1 and insulin co-staining of a whole-mounted human islet assessed by confocal microscopy; scale bars, 25 μm; bottom images are enlargements of the boxed areas in the top images. (**c**) Intracellular nitrite and ROS in human islets cultured for 2 h in 5.5 mM glucose containing 50 ng ml^{-1} IL-1β, IL-23 or IL-24, 0.5 mM palmitate or 10 μg ml^{-1} of an anti–IL-22R1 antibody ± 50 ng ml^{-1} IL-22 introduced 30 min before the stressors. (**d**,**e**) mRNA expression of oxidative stress (*NOS2*, *SOD2*) (**d**) and ER stress (spliced *XBP1* (s*XBP1*)) (**e**) genes in human islets cultured for 24 h as in **c** except IL-22 was introduced at the same time as the stressors (fold of control). Controls: 0.1% DMSO (left), BSA (middle) and anti-IgG antibody (right). Statistics: in **a**,**b**, single donor HI-5; in **c**: three donors (HI-2, HI-3 and HI-4), mean of three replicate cultures per donor; in **d**,**e**, three donors (HI-2, HI-3 and HI-6), mean of three replicate cultures per donor. Kruskal Wallis nonparametric ANOVA, Dunn's *post hoc* test; $^{*,\#}P < 0.05$, $^{**,\#\#}P < 0.01$, $^{***,\#\#\#}P < 0.001$ (from *post hoc* test); * versus control, # versus paired condition without IL-22.

proinsulin accumulation, there was no change in expression of the prohormone convertase, which processes proinsulin into insulin (**Supplementary Fig. 7e**).

Islets from IgG-treated obese mice showed insulin hypersecretion in response to glucose, which we did not observe in islets from obese mice treated with IL-22 (**Fig. 5c**), replicating the result of *ex vivo* exposure to IL-22 in HFD islets (**Fig. 2e**). Exposure to glucose and GLP-1 resulted in secretion of equal amounts of total insulin by islets from HFDIO, IL-22–treated HFDIO and nonobese mice (**Fig. 5c**). However, whereas islets from nonobese mice did not secrete any detectable proinsulin, islets from HFDIO mice did secrete proinsulin, and islets from obese mice treated *in vivo* with IL-22 had substantially lower proinsulin secretion (**Fig. 5c**).

To assess the functional quality of insulin, we compared the ability of the insulin secreted by islets in response to glucose and GLP-1 to stimulate uptake of fluorescent 6-(*N*-(7-nitrobenz-2-oxa-1,3-diazol-4-yl)amino)-6-deoxyglucose (6-NBDG) by mouse 3T3 cells differentiated into adipocytes. At an equivalent concentration determined by ELISA, insulin secreted by islets from HFDIO mice *ex vivo* stimulated 70% less adipocyte 6-NBDG uptake than insulin secreted by islets from normal chow–fed mice. In contrast, insulin secreted by islets from obese mice treated with 100 ng g^{-1} IL-22 was only 11% less effective than insulin from islets isolated from lean mice (**Fig. 5d**).

Antioxidant genes and *Nos2* were more highly expressed in islets from HFDIO mice, whereas islets from IL-22–treated obese mice had even higher expression of antioxidant genes and lower expression of *Nos2* (**Fig. 5e**), emulating what we observed when we treated beta cells (**Fig. 1i**) and islets (**Fig. 2d**) with IL-22 *in vitro*. ER stress was lower in islets from HFDIO mice treated with both doses of IL-22 than in islets from IgG-treated obese mice, with *Xbp1* splicing islets from mice treated with 100 ng g^{-1} IL-22 indistinguishable from that in islets from mice fed normal chow (**Fig. 5e**). A remaining question was whether IL-22–mediated suppression of ER stress reduced inflammation within islets. Expression of multiple cytokines and chemokines was lower in islets from HFDIO mice treated with IL-22 *in vivo*, with the higher dose generally more efficacious (**Fig. 5e**). Furthermore, mRNA expression of multiple chemokines was reduced substantially in HFDIO islets cultured in IL-22 (**Fig. 5f**), paralleling lower ER stress (**Fig. 2d**).

IL-22 protects human islets from oxidative and ER stress

In order to ascertain whether human beta cells are similarly affected by IL-22, we obtained human islets from healthy organ donors. Using flow cytometry (**Fig. 6a**) and confocal microscopy (**Fig. 6b** and **Supplementary Fig. 8a**), we were able to replicate previous findings of high IL-22R1 expression by human beta cells[25].

We cultured islets from three donors in the presence of IL-1β, IL-23, IL-24, palmitate or an IL-22R1–neutralizing antibody, with or without exposure to IL-22. After 2 h, IL-1β initiated the greatest ROS production, whereas IL-24 stimulated the most nitrite (a dose-response curve for one donor is shown in **Supplementary Fig. 8b**). However, a 30-min pre-exposure to IL-22 largely prevented the production of ROS and nitrite in response to all of the cytokines and palmitate (**Fig. 6c**). The IL-22R1–neutralizing antibody induced substantial production of both ROS and nitrite (**Fig. 6c**), indicating that endogenous IL-22 is also a key component of oxidative homeostasis in human islets. We also exposed islets to IL-1β, IL-24, palmitate or the IL-22R1–neutralizing antibody for 24 h, with or without concomitant exposure to IL-22, and assessed expression of oxidative stress and ER stress genes. *NOS2* (iNOS) expression was lower in nonstressed islets cultured in IL-22 and was induced by the stressors, with IL-24 driving the highest gene expression (mean 10.1-fold higher). Co-culture with IL-22 largely prevented *NOS2* induction (**Fig. 6d**). Across all conditions in the two donors with both measures there was a strong correlation between nitrite production and *NOS2* gene expression ($r = 0.72$, $P = 0.0002$). Mean *SOD2* expression was 7.1-fold higher in human islets cultured in IL-22, and this high expression was maintained in cells cocultured with IL-1β, IL-24 or palmitate (**Fig. 6d**). The cytokines and palmitate induced ER stress, as determined by spliced *XBP1* mRNA levels, and this was prevented by IL-22 (**Fig. 6e**). Consistent with the induction of ROS and nitrite, the IL-22R1–neutralizing antibody also caused substantial ER stress (*sXBP1* mean 8.3-fold higher) (**Fig. 6e**). Titration

experiments showed that the half-maximum inhibitory concentrations (IC_{50}s) for inhibition of palmitate-induced nitrite production, *NOS2* induction and *XBP1* splicing by IL-22 were 4.0, 3.8 and 2.2 ng ml^{-1}, respectively (**Supplementary Fig. 8c–e**) which is similar to the IC_{50} of 2.2 ng ml^{-1} for suppression of IL-23–induced ER stress in the mouse insulinoma cells (**Fig. 1b**). We conducted a pharmacokinetic experiment in mice administered the 100 ng g^{-1} dose of IL-22 and found a peak serum concentration (2.2 ng ml^{-1}) close to the effective *in vitro* concentration, with almost complete clearance within 60 min (**Supplementary Fig. 8f**).

DISCUSSION

We demonstrate that IL-22 is a powerful endogenous paracrine suppressor of oxidative and ER stress in pancreatic islets and that in obesity-induced hyperglycemia IL-22 therapy restores glucose control by attenuating defects in beta cell insulin biosynthesis and secretion. IL-22 prevents oxidative and ER stress in mouse and human beta cells, whether the stress is induced by lipids, inflammatory cytokines or environmental ROS, via STAT1- and STAT3-mediated upregulation of antioxidant genes and suppression of oxidative stress–inducing genes. In obese mice, IL-22 administration had multiple highly desirable physiological consequences, including restoration of glucose tolerance, resolution of hyperinsulinemia and hyperproinsulinemia, restitution of insulin sensitivity, decreased body weight and redistribution of fat to healthy depots. Similar beneficial effects of administration of an IL-22–Fc fusion protein on metabolic disease were recently also described in mouse HFD-induced and leptin receptor–deficient obesity, and these were ascribed to multiple extrapancreatic effects of IL-22 (ref. 30). In addition to the effect of IL-22 on beta cells, we demonstrate that several innate cytokines not previously linked with T2D are potent inducers of beta cell oxidative and ER stress and contribute to impaired glycemic control. Together, these findings open new approaches for diabetes therapy with potential to control hyperglycemia and preserve beta cells.

Our experiments indicate development of a forward-feeding cycle of oxidative stress, ER stress and inflammation within islets in obesity that is reversible upon appropriate therapy. Although there are multiple contributors to beta cell oxidative and ER stress in obesity, we show there are multiple cytokines in islets that exacerbate ER stress. Our experiments confirm that ER stress leads to inflammatory signaling[8,14,31–33] and show that alleviation of oxidative and ER stress with IL-22 suppresses islet chemokine production. We propose the balance between stress-promoting factors and IL-22 determines the level of beta cell stress, the fidelity of insulin biosynthesis and secretion, and glucose homeostasis. This appears finely tuned, as blocking endogenous IL-22 signaling in mouse and human islets induced oxidative stress, and, although exogenous stressors could overwhelm endogenous IL-22, exogenous IL-22 concentrations above 4 ng ml^{-1} gave substantial protection. IL-22–producing T cells, natural killer cells and innate lymphoid cells have been reported in whole pancreas[34], but not specifically within islets. Although we show *Il22* mRNA in islets, the relative contribution of specific immune cell types and the regulation of their IL-22 production remains to be determined, and cells other than leukocytes could produce IL-22. Our observation that blocking IL-22R1 signaling causes beta cell oxidative stress is consistent with the recent demonstration that *Il22ra1*$^{-/-}$ mice are susceptible to diabetes[30]. However, the same study found unchanged diabetes susceptibility in *Il22*$^{-/-}$ mice[30], raising a possibility that an alternative IL-22R1 ligand can suppress islet oxidative stress. IL-20 and IL-24 can signal via an IL-22R1–IL-20R2 heterodimer, but administration of IL-20 or IL-24 did not ameliorate metabolic disease in mice[30], and we show that IL-24 promotes beta cell stress and metabolic disease.

IL-22 therapy is also likely to diminish ER stress–induced beta cell apoptosis, a key feature of diabetes progression[35]. The partial efficacy of IL-23– and IL-24–neutralizing antibodies in mice, and the modest efficacy of IL-1β antagonism in clinical trials[17–22], is consistent with there being multiple contributors to beta cell stress. Although it is possible that the lower efficacy of the therapeutic antibodies in our experiments could also be related to incomplete cytokine neutralization, the greater efficacy of IL-22 is consistent with our demonstration that IL-22 suppresses stress initiated by multiple cytokines, glucolipotoxicity and environmental ROS.

Low levels of ROS may be important in signal transduction and regulatory processes in beta cells[36]. However, high intracellular concentrations of ROS and NOS induce protein misfolding by disturbing the ER redox state, disrupting disulfide bond formation and reduction, by nitrosylating peptides and by disturbing ER Ca^{2+} retention[37,38]. The oxidative stress pathway genes regulated by IL-22 have the capability to decrease intracellular concentrations of O_2^-, H_2O_2, NO, OH and $ONOO^-$, plausibly explaining how IL-22 prevents ER stress. Downregulation of iNOS will limit production of NO, a mediator of the beta cell response to cytokines, NEFAs and high glucose and a trigger for apoptosis[10,39]. IL-22 upregulated Sod2, which converts O_2^- to H_2O_2 in mitochondria, and Gpx5 and Prdx5, which catalyze the conversion of H_2O_2 to H_2O. H_2O_2 and NO can react to form peroxynitrite ($ONOO^-$), which contributes to protein misfolding[40] and beta cell apoptosis[41]. Prdx5 highly efficiently reduces peroxynitrite[42]. Conversely, Hsp90ab1, which was downregulated by IL-22, is required for NEFA-induced mitochondrial peroxynitrite production[43]. Downregulation of Fth1 may limit the availability of Fe^{3+} for catalysis of reactions in oxidative stress pathways. IL-22 increased *Cyba* levels but not mRNA levels of genes encoding the catalytic Nox proteins, which convert O_2 to O_2^-. IL-22 regulates these genes in the absence of oxidative stress, thereby protecting beta cells from subsequent stressors, distinguishing IL-22 from the Keap1-Nrf2 system, which is induced by oxidative stress[44].

In obesity *in vivo* and *ex vivo*, IL-22 suppressed islet oxidative and ER stress, set an appropriate level of insulin secretion in response to glucose and GLP-1, reduced proinsulin secretion and improved the quality of secreted insulin. Our finding that 4 weeks of IL-22 therapy restores insulin sensitivity in obese mice is supported by a recent study[30]. However, we show that glycemic control precedes resolution of insulin resistance, suggesting the improved glucose control in obese mice is primarily due to suppression of beta cell stress and restoration of appropriate insulin biosynthesis and secretion. Inhibition of insulin secretion during acute ER stress probably ensues from inhibition of translation[26] and ER retention of the Wolfram syndrome 1 protein, which moves from the ER to the cytoplasm in response to high glucose, complexes with and activates adenylyl cyclase 8, and thereby promotes cAMP production and insulin secretion[6]. Whereas alleviation of acute ER stress by IL-22 increased insulin secretion, in obese islets adapted to chronic ER stress and inflammation, IL-22 decreased insulin hypersecretion and diminished proinsulin accumulation and secretion. Circulating glucose and insulin concentrations following glucose challenge in IL-22–treated obese mice in our experiments, and in a recent report[30], were completely consistent with secretion of less, but more effective, insulin. Reduced insulin and proinsulin secretion upon glucose and GLP-1 challenge was also observed in *ex vivo* culture of islets from IL-22–treated mice and when islets from obese mice were treated *in vitro* with IL-22. The improved glycemic

control with less secreted insulin observed in IL-22–treated mice, despite unchanged insulin resistance, is consistent with the greater efficacy of the insulin secreted by islets taken from these mice to drive adipocyte glucose uptake.

Although our data show that IL-22 directly affects beta cells, IL-22 may have additional benefits via other IL-22R1–expressing cells. Leukocytes are generally considered to lack IL-22R1, making direct effects of IL-22 on immune cells unlikely, although a recent study reports IL-22R1 expression on adipose tissue macrophages[45]. Previous studies of IL-22 administration in obesity report decreased hepatic lipogenesis, lowered hepatic triglyceride and cholesterol concentrations [46] and diminished hepatic triglyceride and serum liver enzyme levels[30], and we show suppressed hepatic upregulation of Grp78. It is not possible to discern whether these responses ensue from direct effects of IL-22 on hepatocytes or are secondary to restoration of glucose tolerance. Of relevance, IL-23–specific and IL-24–specific antibodies partially improved glucose tolerance and partially suppressed hepatic Grp78 expression. IL-22, IL-20 and IL-24 increased expression of lipid metabolism genes in adipocytes, but IL-20 and IL-24 could not resolve metabolic disease[30]. Islet alpha cells also express IL-22R1 and are susceptible to ER stress[47] that we show is alleviated by IL-22. The major product of alpha cells, glucagon, induces hepatic gluconeogenesis, and hyperglucagonemia is a hallmark of T2D. Regulation of glucagon secretion involves both alpha cell–intrinsic pathways and paracrine regulation such as the suppression by insulin[48]. Although we saw no changes in serum glucagon, we cannot exclude reduced alpha cell oxidative and ER stress and improved efficacy of beta cell–derived insulin to control glucagon release contributing to improved glucose homeostasis in IL-22–treated mice.

In our experiments, IL-22 reduced body weight after blood glucose began to fall. A recent study showed that IL-22–mediated weight loss is potentially explained by increased serum concentrations of the gut-derived anorectic hormone PYY[30]. However, pairwise feeding experiments demonstrated that reduced food consumption could not explain the improved glucose tolerance[30]. IL-22 has been linked with regulation of microbial populations in obesity in the context of lymphotoxin deficiency, where hydrodynamic transfection of IL-22 increased body weight[49]. Consistent with IL-22 therapy in acute mouse pancreatitis[34], we show reduced pancreatic acinar cell ER stress after IL-22, which may alter the secretion of digestive enzymes, the absorption of calories and the gut microbiota, potentially contributing to weight loss. IL-22 may also alleviate oxidative and ER stress in intestinal mucus-producing goblet cells (as we showed for IL-10 (ref. 50)) and enteroendocrine cells, which secrete incretins and appetite-regulating hormones, including PYY. Mucus influences intestinal microbial populations, and one study has attributed the microbial changes in diabetes that affect systemic metabolism to goblet cell ER stress[51]. In colitis, increased mucin production in response to IL-22 has been attributed to induction of mucin genes[52], but suppression of ER stress may be important. In summary, IL-22 may have multiple positive influences on metabolic disease, but the primary rapid improvement in glucose homeostasis is consistent with the direct effects on beta cells that we describe.

Given the favorable effects of exogenous IL-22 and the fact that there are fewer IL-22–producing lymphocytes in mouse obesity, it has been proposed that reduced endogenous IL-22 contributes to metabolic syndrome[30]. In contrast, we found increased *Il22* mRNA within islets of obese mice. Also contrasting with the report of reduced T cell IL-22 production in mice, in human obesity there is an increased frequency of IL-22–expressing $CD4^+$ T cells in peripheral blood and adipose tissue and modest increases in serum IL-22 (refs. 45,53,54). Nevertheless, the highest serum IL-22 concentrations in obese humans (<80 pg ml^{-1}) are well below the IC_{50} for IL-22 suppression of oxidative stress in human islets (2-4,000 pg ml^{-1}) and thus are unlikely to influence islet function. A study showing that exogenous IL-22 reduces insulin-mediated glucose uptake in muscle used very high concentrations of IL-22 unlikely to be reached in muscle[53]. Transgenic overexpression of IL-22 in mouse adipose tissue induced local inflammation and lipomas in mice on an HFD but only achieved serum concentrations of <10 pg ml^{-1} and had no impact on glucose intolerance or insulin resistance[55]. The paracrine effects of IL-22 are likely to be most important, as will be local concentrations of the soluble IL-22 binding protein (IL-22RA2), which is most highly expressed in skin and intestine[56].

In human T2D, therapeutic modulation of the ER stress–regulating cytokines, the cells that produce them, or their downstream signaling pathways has the potential to restore beta cell function and reduce beta cell depletion, thus helping constrain disease progression. IL-22 therapy looks promising but may have risks because high local concentrations of IL-22 contribute to pathology in psoriasis[57], and IL-22 promotes intestinal proliferation and could contribute to inflammation-driven neoplasia[55,58]. However, we saw no histological or morphological effects on the skin or gut with our intermittent short-acting doses. Adverse effects were also not reported following administration of an IL-22–Fc fusion protein with a half-life of ~3 d, administered twice weekly at approximately three- to sixfold higher molar concentrations than our maximal dose[30]. Optimal efficacious, but nontoxic, dosing schedules for IL-22 remain to be determined.

We demonstrate direct receptor-mediated mechanisms by which cytokines regulate beta cell insulin biosynthesis and secretion via control of oxidative and ER stress. The multiple pathways used by immunity to disrupt secretory protein biosynthesis, although probably advantageous during infections, cause pathology in the chronic pancreatic inflammation in obesity and T2D. In autoimmune type 1 diabetes, beta cell ER stress has been demonstrated at diagnosis[59], and in the NOD mouse model of autoimmune diabetes beta cell ER stress precedes insulitis[60]. IL-22 therapy in type 1 diabetes could protect beta cells by reducing oxidative and ER stress. Human islets for transplantation may benefit from culture in IL-22, and IL-22 therapy in recipients may aid establishment and function of islets. Beyond diabetes, we suggest that the immune regulation of ER stress has relevance to infectious, inflammatory and protein misfolding diseases.

METHODS

Methods and any associated references are available in the online version of the paper.

Note: Any Supplementary Information and Source Data files are available in the online version of the paper.

ACKNOWLEDGMENTS

We would like to thank the staff of the Mater Research and Translational Research Institute Biological Research Facilities for care of experimental animals, L. Crowley and S. Roy for assistance with confocal microscopy, H. Nielsen for technical assistance with immunofluorescence staining, and A. Bertolotti and D. Serisier for discussions about the manuscript. J.M.F., J.P.W. and M.A.M. are or were supported by Australian National Health and Medical Research Council Senior Research Fellowships. The research was supported by Australian National Health and Medical Research Council Project Grant 1047905 and the Mater Foundation. MIN6N8 cells were a kind gift from J. Miyazaki, Osaka University. F-*XBP1*ΔDBD-*venus* was a kind gift from M. Miura, University of Tokyo. Anti–IL-23 was a gift from Eli-Lilly.

AUTHOR CONTRIBUTIONS

S.Z.H., J.M.F., J.P.W., J.B.P. and M.A.M. developed the concept, designed the experiments, interpreted the data and wrote the manuscript. S.Z.H. was involved in

all the experimental work and data analysis. D.J.B. conducted studies with mouse islets. B.E.H. conducted the studies in db/db mice. H.T., C.P.N., I.D., R.W. and A.C.-H.C. conducted experiments in HFD mice. T.L., T.W.K. and H.E.T. isolated human islets and contributed to experiments with human islets. Y.H.S. conducted flow cytometry experiments. B.E.H., D.J.B., H.T., Y.H.S., C.P.N., I.D., R.W., A.C.-H.C., T.L., T.W.K. and H.E.T. contributed to redrafting of the manuscript.

COMPETING FINANCIAL INTERESTS

The authors declare no competing financial interests.

Reprints and permissions information is available online at http://www.nature.com/reprints/index.html.

1. Ashcroft, F.M. & Rorsman, P. Diabetes mellitus and the beta cell: the last ten years. *Cell* **148**, 1160–1171 (2012).
2. Back, S.H. & Kaufman, R.J. Endoplasmic reticulum stress and type 2 diabetes. *Annu. Rev. Biochem.* **81**, 767–793 (2012).
3. Cnop, M., Foufelle, F. & Velloso, L.A. Endoplasmic reticulum stress, obesity and diabetes. *Trends Mol. Med.* **18**, 59–68 (2012).
4. Donath, M.Y. & Shoelson, S.E. Type 2 diabetes as an inflammatory disease. *Nat. Rev. Immunol.* **11**, 98–107 (2011).
5. Volchuk, A. & Ron, D. The endoplasmic reticulum stress response in the pancreatic beta-cell. *Diabetes Obes. Metab.* **12** (suppl. 2), 48–57 (2010).
6. Fonseca, S.G., Urano, F., Weir, G.C., Gromada, J. & Burcin, M. Wolfram syndrome 1 and adenylyl cyclase 8 interact at the plasma membrane to regulate insulin production and secretion. *Nat. Cell Biol.* **14**, 1105–1112 (2012).
7. Hasnain, S.Z., Lourie, R., Das, I., Chen, A.C. & McGuckin, M.A. The interplay between endoplasmic reticulum stress and inflammation. *Immunol. Cell Biol.* **90**, 260–270 (2012).
8. Menu, P. *et al.* ER stress activates the NLRP3 inflammasome via an UPR-independent pathway. *Cell Death Dis.* **3**, e261 (2012).
9. Chan, J.Y., Biden, T.J. & Laybutt, D.R. Cross-talk between the unfolded protein response and nuclear factor-κB signalling pathways regulates cytokine-mediated beta cell death in MIN6 cells and isolated mouse islets. *Diabetologia* **55**, 2999–3009 (2012).
10. Kacheva, S., Lenzen, S. & Gurgul-Convey, E. Differential effects of proinflammatory cytokines on cell death and ER stress in insulin-secreting INS1E cells and the involvement of nitric oxide. *Cytokine* **55**, 195–201 (2011).
11. Gurzov, E.N. *et al.* Signaling by IL-1β+IFN-γ and ER stress converge on DP5/Hrk activation: a novel mechanism for pancreatic beta-cell apoptosis. *Cell Death Differ.* **16**, 1539–1550 (2009).
12. Ghosh, R. *et al.* Allosteric Inhibition of the IRE1α RNase preserves cell viability and function during endoplasmic reticulum stress. *Cell* **158**, 534–548 (2014).
13. Lee, A.H., Heidtman, K., Hotamisligil, G.S. & Glimcher, L.H. Dual and opposing roles of the unfolded protein response regulated by IRE1α and XBP1 in proinsulin processing and insulin secretion. *Proc. Natl. Acad. Sci. USA* **108**, 8885–8890 (2011).
14. Oslowski, C.M. *et al.* Thioredoxin-interacting protein mediates ER stress-induced beta cell death through initiation of the inflammasome. *Cell Metab.* **16**, 265–273 (2012).
15. Lerner, A.G. *et al.* IRE1α induces thioredoxin-interacting protein to activate the NLRP3 inflammasome and promote programmed cell death under irremediable ER stress. *Cell Metab.* **16**, 250–264 (2012).
16. Chen, J., Fontes, G., Saxena, G., Poitout, V. & Shalev, A. Lack of TXNIP protects against mitochondria-mediated apoptosis but not against fatty acid–induced ER stress–mediated beta-cell death. *Diabetes* **59**, 440–447 (2010).
17. Larsen, C.M. *et al.* Interleukin-1-receptor antagonist in type 2 diabetes mellitus. *N. Engl. J. Med.* **356**, 1517–1526 (2007).
18. Moran, A. *et al.* Interleukin-1 antagonism in type 1 diabetes of recent onset: two multicentre, randomised, double-blind, placebo-controlled trials. *Lancet* **381**, 1905–1915 (2013).
19. Rissanen, A., Howard, C.P., Botha, J. & Thuren, T. Effect of anti-IL-1β antibody (canakinumab) on insulin secretion rates in impaired glucose tolerance or type 2 diabetes: results of a randomized, placebo-controlled trial. *Diabetes Obes. Metab.* **14**, 1088–1096 (2012).
20. Ridker, P.M. *et al.* Effects of interleukin-1β inhibition with canakinumab on hemoglobin A1c, lipids, C-reactive protein, interleukin-6, and fibrinogen: a phase IIb randomized, placebo-controlled trial. *Circulation* **126**, 2739–2748 (2012).
21. Cavelti-Weder, C. *et al.* Effects of gevokizumab on glycemia and inflammatory markers in type 2 diabetes. *Diabetes Care* **35**, 1654–1662 (2012).
22. Sloan-Lancaster, J. *et al.* Double-blind, randomized study evaluating the glycemic and anti-inflammatory effects of subcutaneous LY2189102, a neutralizing IL-1β antibody, in patients with type 2 diabetes. *Diabetes Care* **36**, 2239–2246 (2013).
23. Iwawaki, T., Akai, R., Kohno, K. & Miura, M. A transgenic mouse model for monitoring endoplasmic reticulum stress. *Nat. Med.* **10**, 98–102 (2004).
24. Cunha, D.A. *et al.* Initiation and execution of lipotoxic ER stress in pancreatic beta-cells. *J. Cell Sci.* **121**, 2308–2318 (2008).
25. Shioya, M., Andoh, A., Kakinoki, S., Nishida, A. & Fujiyama, Y. Interleukin 22 receptor 1 expression in pancreas islets. *Pancreas* **36**, 197–199 (2008).
26. Harding, H.P., Zhang, Y. & Ron, D. Protein translation and folding are coupled by an endoplasmic-reticulum-resident kinase. *Nature* **397**, 271–274 (1999).
27. Mahdi, T. *et al.* Secreted frizzled-related protein 4 reduces insulin secretion and is overexpressed in type 2 diabetes. *Cell Metab.* **16**, 625–633 (2012).
28. Cobleigh, M.A. & Robek, M.D. Protective and pathological properties of IL-22 in liver disease: implications for viral hepatitis. *Am. J. Pathol.* **182**, 21–28 (2013).
29. Malhi, H. & Kaufman, R.J. Endoplasmic reticulum stress in liver disease. *J. Hepatol.* **54**, 795–809 (2011).
30. Wang, X. *et al.* Interleukin-22 alleviates metabolic disorders and restores mucosal immunity in diabetes. *Nature* 10.1038/nature13564 (6 August 2014).
31. Igoillo-Esteve, M. *et al.* Palmitate induces a pro-inflammatory response in human pancreatic islets that mimics CCL2 expression by beta cells in type 2 diabetes. *Diabetologia* **53**, 1395–1405 (2010).
32. Kaneko, M., Niinuma, Y. & Nomura, Y. Activation signal of nuclear factor-κB in response to endoplasmic reticulum stress is transduced via IRE1 and tumor necrosis factor receptor-associated factor 2. *Biol. Pharm. Bull.* **26**, 931–935 (2003).
33. Pahl, H.L. & Baeuerle, P.A. Activation of NF-κB by ER stress requires both Ca^{2+} and reactive oxygen intermediates as messengers. *FEBS Lett.* **392**, 129–136 (1996).
34. Xue, J., Nguyen, D.T. & Habtezion, A. Aryl hydrocarbon receptor regulates pancreatic IL-22 production and protects mice from acute pancreatitis. *Gastroenterology* **143**, 1670–1680 (2012).
35. Papa, F.R. Endoplasmic reticulum stress, pancreatic beta-cell degeneration, and diabetes. *Cold Spring Harb. Perspect. Med.* **2**, a007666 (2012).
36. Newsholme, P. *et al.* Reactive oxygen and nitrogen species generation, antioxidant defenses, and beta-cell function: a critical role for amino acids. *J. Endocrinol.* **214**, 11–20 (2012).
37. Malhotra, J.D. & Kaufman, R.J. Endoplasmic reticulum stress and oxidative stress: a vicious cycle or a double-edged sword? *Antioxid. Redox Signal.* **9**, 2277–2293 (2007).
38. Cardozo, A.K. *et al.* Cytokines downregulate the sarcoendoplasmic reticulum pump Ca^{2+} ATPase 2b and deplete endoplasmic reticulum Ca^{2+}, leading to induction of endoplasmic reticulum stress in pancreatic beta-cells. *Diabetes* **54**, 452–461 (2005).
39. Bedoya, F.J. *et al.* Regulation of pancreatic beta-cell survival by nitric oxide: clinical relevance. *Islets* **4**, 108–118 (2012).
40. Dickhout, J.G. *et al.* Peroxynitrite causes endoplasmic reticulum stress and apoptosis in human vascular endothelium: implications in atherogenesis. *Arterioscler. Thromb. Vasc. Biol.* **25**, 2623–2629 (2005).
41. Hou, R. *et al.* Upregulation of PTEN by peroxynitrite contributes to cytokine-induced apoptosis in pancreatic beta-cells. *Apoptosis* **15**, 877–886 (2010).
42. Knoops, B., Goemaere, J., Van der Eecken, V. & Declercq, J.P. Peroxiredoxin 5: structure, mechanism, and function of the mammalian atypical 2-Cys peroxiredoxin. *Antioxid. Redox Signal.* **15**, 817–829 (2011).
43. Zhang, H.M., Dang, H., Yeh, C.K. & Zhang, B.X. Linoleic acid-induced mitochondrial Ca^{2+} efflux causes peroxynitrite generation and protein nitrotyrosylation. *PLoS ONE* **4**, e6048 (2009).
44. Bryan, H.K., Olayanju, A., Goldring, C.E. & Park, B.K. The Nrf2 cell defence pathway: Keap1-dependent and -independent mechanisms of regulation. *Biochem. Pharmacol.* **85**, 705–717 (2013).
45. Dalmas, E. *et al.* T cell-derived IL-22 amplifies IL-1β-driven inflammation in human adipose tissue: relevance to obesity and type 2 diabetes. *Diabetes* **63**, 1966–1977 (2014).
46. Yang, L. *et al.* Amelioration of high fat diet induced liver lipogenesis and hepatic steatosis by interleukin-22. *J. Hepatol.* **53**, 339–347 (2010).
47. Akiyama, M. *et al.* X-box binding protein 1 is essential for insulin regulation of pancreatic alpha cell function. *Diabetes* **62**, 2439–2449 (2013).
48. Walker, J.N. *et al.* Regulation of glucagon secretion by glucose: paracrine, intrinsic or both? *Diabetes Obes. Metab.* **13** (suppl. 1), 95–105 (2011).
49. Upadhyay, V. *et al.* Lymphotoxin regulates commensal responses to enable diet-induced obesity. *Nat. Immunol.* **13**, 947–953 (2012).
50. Hasnain, S.Z. *et al.* IL-10 promotes production of intestinal mucus by suppressing protein misfolding and endoplasmic reticulum stress in goblet cells. *Gastroenterology* **144**, 357–368 (2013).
51. Wei, X. *et al.* Fatty acid synthase modulates intestinal barrier function through palmitoylation of mucin 2. *Cell Host Microbe* **11**, 140–152 (2012).
52. Sugimoto, K. *et al.* IL-22 ameliorates intestinal inflammation in a mouse model of ulcerative colitis. *J. Clin. Invest.* **118**, 534–544 (2008).
53. Fabbrini, E. *et al.* Association between specific adipose tissue $CD4^+$ T-cell populations and insulin resistance in obese individuals. *Gastroenterology* **145**, 366–374 e1–3 (2013).
54. Zhao, R. *et al.* Elevated peripheral frequencies of T_H22 cells: a novel potent participant in obesity and type 2 diabetes. *PLoS ONE* **9**, e85770 (2014).
55. Wang, Z. *et al.* High fat diet induces formation of spontaneous liposarcoma in mouse adipose tissue with overexpression of interleukin 22. *PLoS ONE* **6**, e23737 (2011).
56. Huber, S. *et al.* IL-22BP is regulated by the inflammasome and modulates tumorigenesis in the intestine. *Nature* **491**, 259–263 (2012).
57. Zheng, Y. *et al.* Interleukin-22, a T_H17 cytokine, mediates IL-23–induced dermal inflammation and acanthosis. *Nature* **445**, 648–651 (2007).
58. Kirchberger, S. *et al.* Innate lymphoid cells sustain colon cancer through production of interleukin-22 in a mouse model. *J. Exp. Med.* **210**, 917–931 (2013).
59. Marhfour, I. *et al.* Expression of endoplasmic reticulum stress markers in the islets of patients with type 1 diabetes. *Diabetologia* **55**, 2417–2420 (2012).
60. Tersey, S.A. *et al.* Islet beta-cell endoplasmic reticulum stress precedes the onset of type 1 diabetes in the nonobese diabetic mouse model. *Diabetes* **61**, 818–827 (2012).

ONLINE METHODS

MIN6N8 cells and assessments of ER/oxidative stress. We maintained MIN6N8 cells (a kind gift from J. Miyazaki, Osaka University) as previously described[61], and they tested negative for mycoplasma. We routinely cultured MIN6N8 cells in phenol-red–free DMEM (Life Technologies) containing 25 mM glucose (3.4 g L^{-1} sodium bicarbonate, 50 U mL^{-1} penicillin and streptomycin, 71.5 μM β-mercaptoethanol and 10% heat-inactivated FBS) and transferred them to DMEM as above with 5.5 mM glucose 48 h before experimentation. We transfected MIN6N8 cells with the ERAI reporter plasmid (F-*XBP1*ΔDBD-*venus*, a kind gift from M. Miura, University of Tokyo)[23] or ATF6-GFP plasmid (Adgene) using Lipofectamine 2000 according to the manufacturer's instructions. For ERAI there was negligible fluorescence in the absence of ER stressors, but upon induction of ER stress, splicing of *XBP1* mRNA by IRE1α results in the translation of Venus but not an active form of XBP1. We measured fluorescence (excitation: 485 nm; emission: 520 nm) using a POLARstar Omega plate reader and treated cells 48 h after transfection. We assessed activation of ATF6 as per the Histology section below. We determined phosphorylation of Ser-51 of eiF2α using an AlphaScreen assay as per the manufacturer's instructions (PerkinElmer). To assess the intracellular concentrations of nitrite (the stable metabolite of nitric oxide), we used the Griess Reagent Kit for Nitrite Determination according to the manufacturer's instructions (Molecular Probes) using lysates of beta cells or islets prepared in RIPA buffer (150 mM NaCl, 1% NP40, 0.5% sodium deoxycholate, 0.1% SDS, 50 mM Tris, pH 7.5). We used the 5-(and-6)-carboxy-2,7-dichlorofluorescein diacetate (DCFDA) assay to determine the concentrations of ROS as previously described[62]. We cultured beta cells and islets in serum-free medium for at least 5 h before commencement of the oxidative stress experiments. We treated cells with glucose or recombinant cytokines at the concentrations indicated in the figure legends, or with 5 μM thapsigargin (Sigma-Aldrich) or 10 μg ml^{-1} tunicamycin (Sigma-Aldrich) or 0.1–0.5 mM palmitic acid (Sigma-Aldrich) for the times indicated in the legends. We prepared a solution of palmitate-BSA complex based on a published method[63]. We prepared a 100 mM stock solution of sodium palmitate in sterile water by alternating heating and vortexing until the palmitate dissolved; this occurred once the solution reached 70 °C. Immediately after the palmitate dissolved, we added 200 μL of the 100 mM palmitate solution to 3.8 mL of serum-free DMEM containing 5% NEFA-free bovine serum albumin (BSA) to make a 5 mM palmitate solution and shook this solution at 140 r.p.m. at 40 °C overnight. We used an equivalent amount of serum-free DMEM containing 5% NEFA-free BSA as a vehicle control for palmitate. Additional controls also contained 0.1% DMSO equivalent to the maximum concentration as the vehicle used for some of the chemical inhibitors. We inhibited oxidative stress using glutathione-reduced (GSH) at 5 mM, superoxide dismutase 1 (SOD1) (Sigma-Aldrich) at 10 μM or L-NG-monomethyl arginine citrate (L-NMMA) at 10 μM (Cayman Chemical). We determined superoxide generation by using the dihydroethidium (DHE) fluorescent cell-permeable probe (Sigma-Aldrich). We incubated MIN6N8 cells plated at 2×10^6 mL^{-1} with 3 μM DHE and subsequently treated cells with 0.1% DMSO (control), 50 ng ml^{-1} IL-23 for 30 min ± 50 ng ml^{-1} IL-22 at the same time or 30 min before IL-23. To inhibit relevant transcription factors and kinases, we incubated cells with STAT1 inhibitor fludarabine (Merck) at 50 μM, STAT3 inhibitor-VI S31-201 (Santa Cruz) at 50 μM, STAT5 inhibitor 573108 at 50 μM (Merck), JNK (inhibitor V) at 10 μM (Merck), ERK inhibitor FR18020 at 5 μM (Merck) or NFκB inhibitor BAY11-7085 (Cell Signaling) at 20 μM.

siRNA gene silencing. We first transfected MIN6N8 cells with ERAI reporter plasmid as above and then after 48 h when 70–80% confluent used Lipofectamine 2000 according to the manufacturer's instructions to transfect them with 100 nM of either individual or combinations of the following siRNAs: control (#6568; Cell Signaling), *Stat1* (#sc-44124; SantaCruz), *Stat3* (#6354; Cell Signaling), *Stat5* (#sc-29496, SantaCruz), NF-κB p65 (*RelA*) (#6339; Cell Signaling), SAPK/JNK (silences *Jnk1* and *Jnk2*, but not *Jnk3*) (#6233; Cell Signaling) or Erk1/2 (*Mapk3*) siRNA (#6560; Cell Signaling). 36 h after siRNA transfection, cells were treated for 24 h with cytokines as indicated in the figure legends, and fluorescence was measured (excitation: 485 nm; emission: 520 nm) using a POLARstar Omega plate reader. RNA was extracted from identical cultures to assess efficiency of siRNA silencing.

Pancreatic islet isolation and culture. We isolated pancreatic islets from C57BL/6 mice, HFDIO, db/db and dbh mice as previously described[64]. We plated islets at 10 islets per well, cultured them overnight in 5.5 mM glucose and treated them with recombinant mouse cytokines (50 ng ml^{-1}), 10 μg ml^{-1} anti-IL-22R1 (Clone 496514; R&D), 5 μM thapsigargin or 10 μg ml^{-1} tunicamycin for the times indicated in the figure legends. We conducted static glucose-stimulated insulin secretion tests by challenging islets consecutively with 2.8 mM glucose for 30 min, 20 mM glucose for 30 min and in some experiments followed by 100 nM GLP-1 (7–36 active peptide; Sigma-Aldrich) in 20 mM glucose for 30 min. We collected supernatants for insulin and proinsulin secretion measurements, and the islets were homogenized in Trizol for RNA analysis. We obtained approval for procuring and performing experiments with human islets from the Mater Health Services Human Research Ethics Committee. We obtained human pancreatic islets from 5 organ donors via the Tom Mandel Islet Transplant Program in Australia (n = 4) or from Prodo Laboratories (n = 1); see **Supplementary Table 4**. Consent for use of the islets for research was given by relatives of the donors. At the Tom Mandel Islet Transplant Program, we prepared islets within a fully contained Isolator (BioSpherix Xvivo System, Lacona, NY) situated in a clean room facility and using a variation of an established method[65]. We removed pancreata from heart-beating deceased donors and disaggregated them by infusing the ducts with cold collagenase (SERVA, Heidelberg, Germany). We separated dissociated islet and acinar tissue on a continuous Biocoll (Biochrom AG, Berlin) density gradient on a refrigerated apheresis system (Model 2991, COBE Laboratories, Lakewood, CO). We counted purified islets and expressed islet number and mass in terms of islet equivalents (IEQ)[66]. We transported islets as soon as possible after isolation and received them 1–7 d after isolation and immediately placed them into culture in CMRL (5.5 mM glucose) containing 10% FCS and 50 U mL^{-1} penicillin and streptomycin (Life Technologies). Purity of the islet preparations were from 70–99%; therefore, after overnight culture we picked individual islets free from exocrine tissue and established them in culture with an equivalent number and size distribution before exposure to cytokines, palmitate or neutralizing antibodies as per figure legends. For assessments of oxidative stress, we cultured 10–30 islets/well for at least 5 h in serum-free media before exposure to the cytokines or drugs.

Flow cytometry. We disaggregated hand-picked islets with Accutase solution (Life Technologies) for 15 min at 37 °C followed by gentle pipetting to disperse the islets. To assess IL-22R1 expression, we first stained islets with anti-human IL-22Ra1 antibody (R&D systems, clone 305405) or IgG isotype control Ab (R&D systems, clone 11711) 10 μg ml^{-1} for 30 min on ice, and then with anti-mouse IgG-PE (Life Technologies, 2.5 μg ml^{-1}), then washed them, fixed them with Fixation/Permeabilization Buffer (eBioscience) according to the manufacturer's instructions, and then stained them with anti-human proinsulin antibody (R&D systems, clone 253627) or isotype controls at 10 μg ml^{-1} in fixation/permeabilization buffers, and then with anti-mouse-Alexa fluor 488 (Life Technologies, 2.5 μg ml^{-1}). We conducted flow cytometry using a CyAn flow cytometer (Beckman Coulter) and analyzed data using Flo Jo v7.2.2 (Tree Star).

Glucose uptake assay. We differentiated 3T3 cells into adipocytes as previously described[67], and all experiments were carried out on day 8 post-differentiation. We seeded 1×10^4 cells in a black 96-well plate and cultured them in serum-free 2.8 mM glucose media before the addition of insulin. We treated cells for 1 h with 2 ng ml^{-1} recombinant insulin or total insulin from islet secretions at 37 °C as described in figure legends. Subsequently, we incubated cells with 10 μM 6-(*N*-(7-nitrobenz-2-oxa-1,3-diazol-4-yl)amino)-6-deoxyglucose (6-NBDG) (Molecular Probes) for 20 min before washing extensively with PBS and determining glucose uptake using a POLARstar Omega plate reader.

Antibodies for *in vitro* studies. We used commercially available polyclonal antibodies against mouse Grp78 (sc-1050, Santa Cruz, dilution 1:100), mouse insulin (#4590; Cell Signaling, dilution 1:500), mouse glucagon (#2760; Cell Signaling, dilution 1:500), mouse proinsulin (clone 253627; R&D Systems, dilution 1:250), mouse PC1/PC3 (#10553; Millipore, dilution 1:100) and human insulin (clone 182410, R&D Systems, dilution 1:500) for immunohistochemistry and immunofluorescence. We used anti-mouse (clone 496514; R&D Systems) and anti-human (clone 305405, R&D Systems) IL-22R1 antibodies at 1:50 and

1:100, respectively, for immunohistochemistry and immunofluorescence, and at 10 μg ml^{-1} for *in vitro* neutralization.

qRT-PCR. We either snap-froze cultured cells, tissue samples and islets first or directly homogenized them in Trizol using FastPrep (MP Biomedical). We isolated RNA using High Pure RNA isolation kit (Roche) or Isolate II RNA Micro Kit (Bioline), followed by cDNA synthesis using iScript (Bio-Rad) or SensiFAST (Bioline) containing oligo(dT) and random hexamers. We used QPCR SYBR Green (Invitrogen) for quantitative PCR using a HT7900 (ABI systems) or Viia7 Real-Time PCR System (Life Technologies) and used RoX as a normalization reference. We analyzed PCR data using SDS software (v2.3) (ABI systems). Primer sequences are included in **Supplementary Table 5**, and we determined efficiencies using cDNA dilutions and primer dilutions for the genes of interest. We normalized all data against the housekeeping genes, *Gapdh* or *GAPDH*, and expressed them as a fold difference to the mean of relevant control samples. We compared cDNA from MIN6N8 cells treated with DMSO or 50 ng ml^{-1} IL-22 for 8 h using the Oxidative Stress RT^2 Profiler PCR Array (Qiagen, PAMM-065Z) and analyzed data using RT^2 Profiler PCR Array data analysis software.

Animal experiments. *High-fat diet induced obesity (HFDIO).* We housed all mice in sterilized, filter-topped cages in a conventional clean facility. We fed 6-8-week-old C57BL/6 male mice *ad libitum* on a high-fat diet containing 46% of available energy as saturated fat, 34% carbohydrate, 20% protein (Specialty feeds, SF04-027) or on normal chow containing less than 10% saturated fat (GoldMix, 126575). HFDIO Experiment 1: From 13-16 weeks of the diet, we treated mice with 20 ng g^{-1} i.p. recombinant mouse IL-22 twice weekly (R&D Systems), 3 μg g^{-1} anti-IL-23 weekly (a gift from Eli Lilly), 0.1 mg/mouse anti-IL-24 weekly (Protein Tech, #12064-1-AP) or 0.5 mg/mouse irrelevant isotype control antibody, and then they were sacrificed and sampled. HFDIO Experiment 2: from 18-22 weeks of diet, we treated mice for 30 d with 20 or 100 ng g^{-1} i.p. recombinant mouse IL-22 twice weekly (R&D Systems) or 100 ng g^{-1} irrelevant isotype control antibody, and then sacrificed and sampled them. We performed fasted i.p. glucose tolerance tests (2 g kg^{-1} glucose) and insulin tolerance tests (0.25 U kg^{-1} insulin; Humalog, Lilly) at the times indicated in the figure legends. We randomly allocated cages of mice to the experimental groups by random draw. We did not blind investigators to treatment, but there were no subjective assessments made.

Leptin deficiency model of diabetes. We sacrificed 20-week-old male diabetic db/db C57BL/KsJ ($Lepr^{+/+}$) and non-diabetic db/h C57BL/KsJ ($Lepr^{+/-}$) mice and collected blood via cardiac puncture. Db/db mice develop severe metabolic defects in the context of type 2 diabetes (hypertension, hyperlipidaemia, obesity, insulin abnormalities). We collected islets from mice in HFDIO experiments and from db/db mice as per the pancreatic islet culture and analysis section. To analyze IL-22 pharmacokinetics, we administered male C57BL/6 mice a single i.p. injection of IL-22 at 100 ng g^{-1} body weight at time 0 and procured blood samples at 15 min intervals over 2 h and at 4 h ($n = 4$ per time point) to determine concentrations of IL-22 in the serum. The only animals that were excluded from analyses were a small number of animals that died unrelated to the treatment in the long-term experiments. All experiments were approved by the University of Queensland Animal Experimentation Ethics Committee or the Alfred Medical Research and Education Precinct Animal Ethics Committee and were conducted in accordance with guidelines set out by the National Health and Medical Research Council of Australia.

ELISA. We measured total insulin and proinsulin in supernatant from islet cultures or in serum from mice using commercially obtained ELISA kits from Millipore and Mercodia, respectively. We determined the molar insulin concentration by subtracting the molar proinsulin concentration from molar total insulin and then calculated the serum proinsulin-insulin ratio. We measured serum glucagon concentrations using an ELISA as per the manufacturer's instructions (R&D Systems, USA). IL-22 was measured in the serum as per manufacturer's intructions (Biolegend; # 436304), with the exception of the assay diluent which was 1% BSA in PBS (pH 7.2).

Histology, immunofluorescence microscopy and histological quantification. We fixed pancreatic tissue in 10% neutral buffered formalin and processed it using standard histological techniques. We used standard immunohistochemical and immunofluorescent staining methods to determine the presence of Grp78, insulin, glucagon, IL-22R1, proinsulin and ATF6-GFP. To quantify ATF6 activation, we determined the area in pixels mm^{-2} with co-localization of ATF6-GFP and DAPI (blue and green) and total ATF6 fluorescence (green) in 5 fields of view for each section using ImageJ software version 1.45s, and then we calculated the percentage of ATF6 and DAPI co-fluorescence to the total ATF6 fluorescence. We determined the area in pixels mm^{-2} for Grp78 and insulin (immunofluorescence) and proinsulin (immunohistochemistry) in the core of the beta cell–rich area of 3–4 islets per mouse using ImageJ software version 1.45s. We carried out live cell imaging in MIN6N8 cells at 37 °C in 5% CO_2 in a chamber using an Olympus xcellence rt microscope. We used time-lapse imaging (3 frames/min for 30 min) to determine the formation of superoxide (DHE-conversion/fluorescence) in cells after treatment and captured DAPI fluorescence to visualize nuclei. We attached isolated human islets to coverslips pre-coated with 0.1 mg ml^{-1} of poly-L-lysine and fixed them in 4% paraformaldehyde/PBS (10 mM, pH 7.2) for 25 min at RT. We washed islets thoroughly with PBS and permeabilized them with 0.3% Triton X-100 in PBS for 3 h. Subsequently, we blocked nonspecific binding with 5% goat serum, 0.15% Triton X-100 in PBS for 2 h at room temperature and then equilibrated islets in 1% BSA, 0.2% Triton X-100 in PBS for 20 min. We diluted the primary and secondary antibodies in 1% BSA, 0.2% Triton X-100 in PBS. We incubated islets with primary antibodies overnight at 4 °C and secondary antibodies for 1 h at room temperature. We subjected whole mounted islets to optical sectioning at 2-μM increments in the *z*-dimension using a Zeiss LSM410 confocal microscope.

Statistical analysis. We powered *in vitro* experiments to see a 2.0 s.d. effect size in a variety of primary outcome measures. The *in vivo* experiments were powered for a 1.5 s.d. change in the area under the curve of the glucose tolerance test as the major primary outcome measure. We performed statistical analyses using GraphPad PRISM version 5.01 (GraphPad software, Inc.) as described in individual figure legends. After confirmation of a normal distribution by probability plots, differences between groups were assessed by using parametric tests (one-way ANOVA with post-test or, where appropriate, a two-tailed Student *t*-test). Where a normal distribution could not be confirmed, we used the Kruskal-Wallis non-parametric ANOVA with a Dunn's *post hoc* test. Correlation was performed using the Spearman rank correlation test.

61. Miyazaki, J. *et al.* Establishment of a pancreatic beta cell line that retains glucose-inducible insulin secretion: special reference to expression of glucose transporter isoforms. *Endocrinology* **127**, 126–132 (1990).
62. Sakon, S. *et al.* NF-kappaB inhibits TNF-induced accumulation of ROS that mediate prolonged MAPK activation and necrotic cell death. *EMBO J.* **22**, 3898–3909 (2003).
63. Zhang, J. *et al.* Measuring energy metabolism in cultured cells, including human pluripotent stem cells and differentiated cells. *Nat. Protoc.* **7**, 1068–1085 (2012).
64. Coughlan, M.T. *et al.* Advanced glycation end products are direct modulators of beta-cell function. *Diabetes* **60**, 2523–2532 (2011).
65. Ricordi, C., Lacy, P.E. & Scharp, D.W. Automated islet isolation from human pancreas. *Diabetes* **38** (suppl. 1), 140–142 (1989).
66. Ricordi, C. *et al.* Islet isolation assessment in man and large animals. *Acta Diabetol. Lat.* **27**, 185–195 (1990).
67. Klemm, D.J. *et al.* Insulin-induced adipocyte differentiation. Activation of CREB rescues adipogenesis from the arrest caused by inhibition of prenylation. *J. Biol. Chem.* **276**, 28430–28435 (2001).

doi:10.1038/nm.3705